RESEARCH ARTICLE | FEBRUARY 21 2019

Simulation of nonlinear system with clearance and analysis of its trajectories FREE

Robert Kostek

AIP Conf. Proc. 2077, 020026 (2019)
https://doi.org/10.1063/1.5091887

Simulation of Nonlinear System with Clearance and Analysis of its Trajectories

Robert Kostek[1, a)]

[1]*University of Science and Technology, Al. Prof. S.Kaliskiego 7, 85-796 Bydgoszcz, Poland*

[a)]Corresponding author: robertkostek@o2.pl

Abstract. This article presents results of simulation of one degree of freedom system with: clearance, linear damping and dry friction. This system models for example machine tools vibrations. Clearance and dry friction introduce strong non-linearity to the studied system. Center and focus are segments, and thus number of equilibrium positions is unlimited. Time histories have characteristic shape, and reveal non-linearity; especially time history of acceleration. Moreover, following trajectories were studied: x-dx/dt, x-d^2x/dt^2, dx/dt-d^2x/dt^2, and 3D x-dx/dt-d^2x/dt^2. They are very useful to identify spring and damping forces and kind of vibrations. These trajectories should be widely employed.

INTRODUCTION

Clearance, dry friction and viscous damping are observed in many mechanical systems. On one hand clearance is required in bearings, because makes movement possible, but on the other hand too large clearance leads to many technical problems; thus is detected and measured. Detection of clearance is a key issue for example in machinery diagnostic. Whereas, dry friction holds elements steady [1,2], can both excite and dump vibrations, and makes precision movement and positioning difficult [3]. Both clearance and dry friction, which are associated with contact mechanics, introduce non-linearity to many mechanical systems, thus are studied in this article.

Clearance leads to discontinuity derivatives of spring characteristic, which finally leads to instability numerical methods based on polynomials; because Runge's phenomenon is observed. Consequently characteristic of suspension system with clearance should not be described with one polynomial. Similar problem is observed for friction force, because friction characteristic is discontinuous and ambiguous for speed being zero dx/dt=0. A few methods can be applied to deal with this instability. First, contact flexibility can be modeled for example with Dahl or Kelvin–Voigt models, then a slider vibrates during stick period [4]. Then, contact can be modeled with viscous damper, consequently system is numerically stable, but numerical creeping is observed. Next, stopping conditions are formulated, and friction force balances forces acting during stick period. Finally, jump discontinuity should not be within integrated interval, which leads to Taylor series method or methods based on Hermite polynomials; because these methods can change easily time step [5]. This shows in short, how to deal with this non-linearity.

Obtained time histories usually are analyzed with FFT (Fast Fourier Transform), which provides an opportunity to find higher harmonics. Higher harmonics inform for example about non-linearity and defects, thus are good state indicators. Nevertheless, spectrum does not provide precise information about reason and kind of non-linearity. Whereas more information about studied system provides trajectories [6]. Classical trajectory is presented in two dimensional space x, dx/dt, but periodically three dimensional trajectories x-dx/dt-d^2x/dt^2 or similar are presented [7-10]. Three dimensional trajectories x-dx/dt-d^2x/dt^2 are presented and interpreted for three systems with clearance. In literature known to author, this issue was not presented in this way.

Scientific Session on Applied Mechanics X
AIP Conf. Proc. 2077, 020026-1–020026-9; https://doi.org/10.1063/1.5091887
Published by AIP Publishing. 978-0-7354-1805-9/$30.00

MODEL OF THE STUDIED SYSTEM

The studied oscillator contains mass, two springs and two dampers. Its movement is described by the following equation of motion:

$$d^2x/dt^2 = (F_s+F_d+F_f) / m \,, \tag{1}$$

where: x denotes displacement m, t time s, F_s spring force N, F_d viscous damping force N, F_f dry friction (damping) force N, and m mass kg. These forces are described by the following equations:

$$F_s = F_{s1}+F_{s2} \,, \tag{2}$$

$$\text{if } x>l \text{ then } F_{s1} = -k_1(x-l) \text{ else } F_{s1} = 0 \,, \tag{3}$$

$$\text{if } x<0 \text{ then } F_{s2} = -k_2 x \quad \text{else } F_{s2} = 0 \,, \tag{4}$$

$$F_d = -c\, dx/dt \,, \tag{5}$$

$$F_f = -F_{fsmax}\, \mathrm{sgn}(dx/dt) \,, \tag{6}$$

where: F_{s1} F_{s2} denote spring forces, k_1 represents stiffness of the first spring N/m, k_2 stiffness of the second spring N/m, l clearance m, c damping coefficient N/(m/s), F_{fsmax} module of the largest friction force N. The studied oscillator is depicted on Fig. 1.

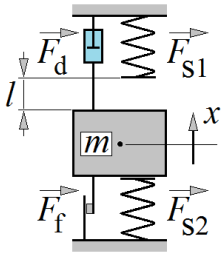

FIGURE 1. Physical model of the studied system.

RESULTS OF SIMULATION

Free Vibrations of System with Clearance

Presented equation of motion (1) can be solved numerically, thus direct method was used [5]. First system with clearance but without any damping was studied, because the simplest system should be analyzed first. Following data were adopted: m=1kg, k_1=k_2=4 N/m, l=1 m, c=0 N/(m/s), F_{fsmax}=0 N, $x_{(t=0)}$=3 m, $dx/dt_{(t=0)}$=0 m/s. Obtained time history of displacement is similar to a harmonic function $x=A\sin(\omega t+\phi)$, which is solution of linear oscillator; nevertheless a straight line segment appears between points A and B (Fig. 2a). This straight line segment represents uniform motion, and is result of clearance. This motion is observed on Fig. 2b as well, while maximal speed is observed. This time period between A and B, which is denoted Δt, changes vibration period T. It should be mentioned, that Δt is a function of maximal speed and clearance, which is described below:

$$dx/dt_{max} = (k_2\, x_{min}^2\, m^{-1})^{0.5} = (k_1\, (x_{max}-l)^2\, m^{-1})^{0.5} \,, \tag{7}$$

$$\Delta t = l \,/\, (dx/dt_{max}) \,,$$

where: Δt denotes time passing clearance. Maximal speed dx/dt_{max} was calculated from law of energy conservation. Then, the exact equation on vibration period can be presented:

$$T = \pi/(k_1\, m^{-1})^{0.5} + \Delta t + \pi/(k_2\, m^{-1})^{0.5} + \Delta t \,, \tag{8}$$

where T denotes vibration period s. These four expressions represent four intervals of motion: contact with the first spring (harmonic motion), two times passing clearance (uniform motion) and contact with the second spring (again harmonic motion). Moreover, the exact solution can be provided for this oscillator (piecewise-defined function). Presented equations show, that for large potential energy Δt can be neglected $\Delta t \to 0$, whereas for small energy Δt plays a significant role. Thus, if $\mathrm{d}x/\mathrm{d}t_{\max} \to 0$ then $\Delta t \to \infty$ and $T \to \infty$. Green areas on Fig. 3c correspond to potential energy. Summarizing this, T is a function of amplitude an energy in this system.

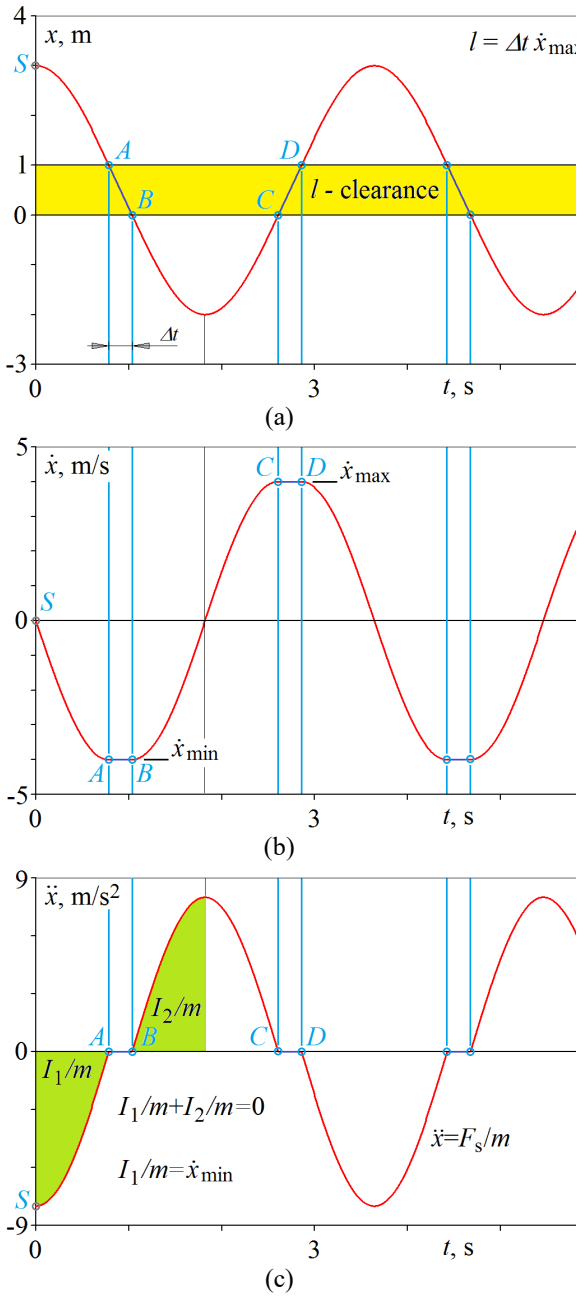

FIGURE 2. Time histories obtained for the system with clearance, calculated for the following data: m=1kg, k_1=k_2=4 N/m, l=1 m, c=0 N/(m/s), F_{fsmax}=0 N, $x_{(t=0)}$=3 m, $\mathrm{d}x/\mathrm{d}t_{(t=0)}$=0 m/s.

Then time history of acceleration can be studied (Fig. 2c). On this graph non-linearity is evident; because no forces are acting in the time interval between A and B, thus $d^2x/dt^2=0$. Summarizing this, horizontal line reflects clearance. Generally, higher derivatives well reveal non-linearity. Moreover, two impulses of forces divided by mass are presented on Fig. 2c. Impulse I_1 causes motion of body ($I_1=m\ dx/dt_{min}$), whereas I_2 stops this motion. This shows, that interesting information can be obtained from the time series.

Next trajectories are studied (Fig. 3). For un-damped linear system trajectories x-dx/dt and dx/dt-d^2x/dt^2 are ellipses, whereas x-d^2x/dt^2 is a straight line segment, moreover center is a point. In contrast to this, for the system with clearance characteristic phenomena are observed. The studied oscillator is un-damped, thus center is observed; in this case center is a straight line segment, thus number of equilibrium positions can not be counted, because is unlimited. Consequently notion of amplitude can not be defined based on an equilibrium position. Moreover all equilibrium positions are neutrally stable (Fig. 3c). Trajectory x-d^2x/dt^2 reflects spring force characteristic $F_s=f(x)$, and energy accumulated by the first E_{S1} and the second spring E_{S2}. These two energies are equal. On this trajectory clearance is evident. Classical trajectory x-dx/dt reveals clearance as well (Fig. 3a), and thus uniform monition is observed between points AB and CD. On the other hand, trajectory dx/dt-d^2x/dt^2 is difficult to interpret, and is a ellipse, because AB segment is projected on one point (Fig. 3d). Phase point circulates round the center, but stops on Δt in AB point. This phenomenon can be observed in animation. Finally, the most interesting is trajectory x-dx/dt-d^2x/dt^2, because presents all described information (Fig. 3b). Point circulates along path $SABCDS$ round center on surface determined by acting forces $d^2x/dt^2=F_s/m$. Unfortunately this trajectory is not commonly used.

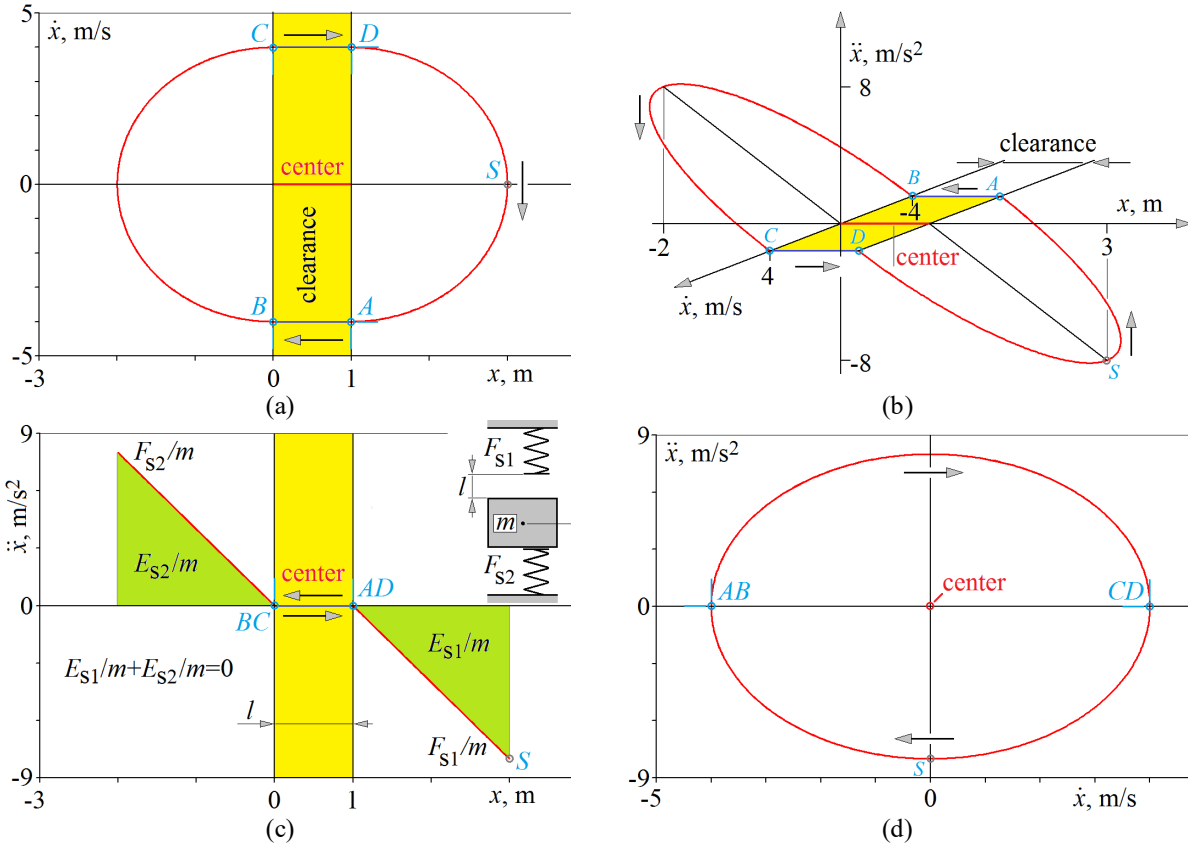

FIGURE 3. Trajectories obtained for the system with clearance, for the following data: m=1kg, $k_1=k_2$=4 N/m, l=1 m, c=0 N/(m/s), F_{fsmax}=0 N, $x_{(t=0)}$=3 m, $dx/dt_{(t=0)}$=0 m/s.

Damped Free Vibrations of System with Clearance and Linear Damping

After the introduction, system with clearance and viscous damping can be studied. Following data were adopted: m=1kg, k_1=k_2=4 N/m, l=1 m, c=0.3 N/(m/s), F_{fsmax}=0 N, $x_{(t=0)}$=3 m, $dx/dt_{(t=0)}$=0 m/s. The time history of displacement shows, that Δt increases with decreasing amplitude of vibration (Fig. 4a). This changes resonance graph, which is not studied in this article. Moreover segments AB, CD and EF are described by exponential functions $x=Ae^{-tc/m}$, because only linear damping force acts on the body at these time intervals.

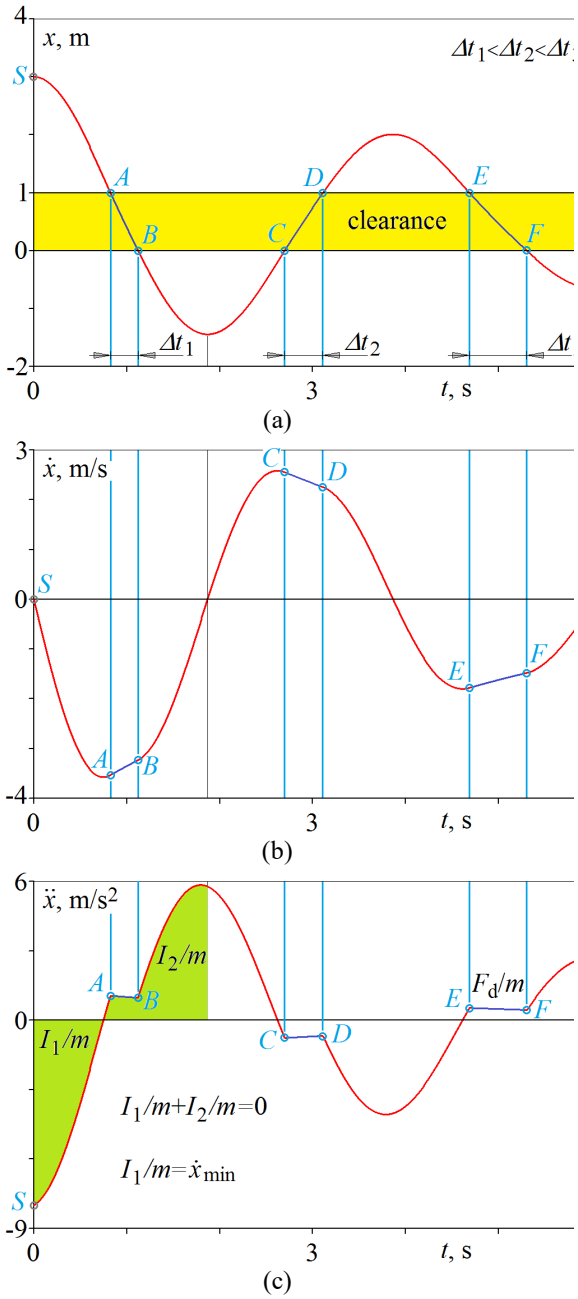

FIGURE 4. Time histories obtained for the system with clearance and linear damping, calculated for the following data: m=1kg, k_1=k_2=4 N/m, l=1 m, c=0.3 N/(m/s), F_{fsmax}=0 N, $x_{(t=0)}$=3 m, $dx/dt_{(t=0)}$=0 m/s.

Whereas segments *SA*, *BC*, *DE* are described by second order linear equation. This shows, that the exact solution is known for selected intervals (piecewise-defined function), thus time history can be calculated with very small error. Summarizing, clearance is difficult to find on this graph. Next time history of velocity is studied (Fig. 4b). In this case extremes are not flat as previously, and have characteristic shape. Finally, the time history of acceleration reveals clearance (Fig. 4c). Characteristic flat segments are near horizontal axis. This is a good state indicator. Moreover two impulses I_1 and I_2 are presented. This shows, that damping changes time histories.

After that, trajectories are studied. For damped linear system trajectories are projections of exponential spiral, but for a system with clearance they have more sophisticated shape. In this case focus is observed, but it is not a point, but is a segment (Fig. 5c). Moreover all equilibrium positions are neutrally stable. Potential energy is dissipated by dumping, hysteresis loop is evident, and thus amplitude drops. Effects of acting forces are observed, and thus the forces can be identified from x-$\mathrm{d}^2x/\mathrm{d}t^2$ trajectory [7]. Moreover energy flow is observed $E_1=E_2$. And *AB, CD* are straight line segments, because damping is linear. This trajectory provides a lot of information (Fig. 5c). Then, x-$\mathrm{d}x/\mathrm{d}t$ trajectory is studied (Fig. 5a). This trajectory contains straight line segments and segments of exponential spiral, moreover has a characteristic shape. Next, $\mathrm{d}x/\mathrm{d}t$-$\mathrm{d}^2x/\mathrm{d}t^2$ trajectory reveals clearance; projection of *AB* segment is not a point, but is a segment, because damping reduces speed and deceleration (Fig. 5d). Segments *AB, EF, DC* are on one straight line $\mathrm{d}^2x/\mathrm{d}t^2 = F_\mathrm{d}/m$. Finally, the most interesting is 3D trajectory x-$\mathrm{d}x/\mathrm{d}t$-$\mathrm{d}^2x/\mathrm{d}t^2$, because presents all provided information (Fig. 5b). Point circulates along path *SABCDEF* round focus on surface determined by acting forces $\mathrm{d}^2x/\mathrm{d}t^2=(F_\mathrm{s}+F_\mathrm{d})/m$. Surface *ABCD* is inclined, because damping force acts. Blue line presents x-$\mathrm{d}x/\mathrm{d}t$ trajectory. This shows, that valuable information is evident on these trajectories.

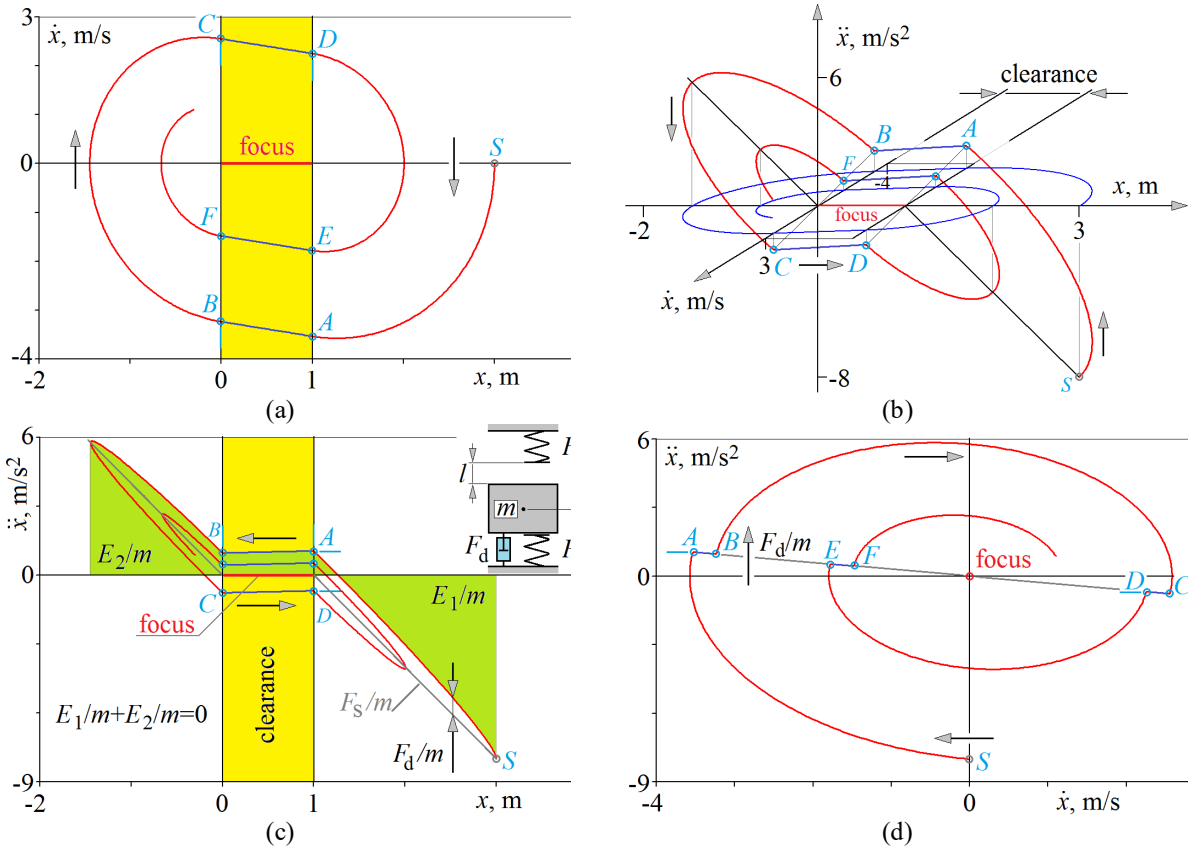

FIGURE 5. Trajectories obtained for the system with clearance and linear damping, for the following data: m=1kg, $k_1=k_2$=4 N/m, l=1 m, c=0.3 N/(m/s), F_{fsmax}=0 N, $x_{(t=0)}$=3 m, $\mathrm{d}x/\mathrm{d}t_{(t=0)}$=0 m/s.

Damped Free Vibrations of System with Clearance and Dry Friction

Finally, system with clearance and Coulomb friction is studied. This system models slide ways and machine tools. Following data were adopted: m=1kg, k_1=k_2=4 N/m, l=1 m, c=0 N/(m/s), F_{fsmax}=0.9 N, $x_{(t=0)}$=3 m, $dx/dt_{(t=0)}$=0 m/s. Time history of displacement shows that, Δt increases with decreasing amplitude of vibration (Fig. 6a). Which changes resonance graph. Moreover segments AB, EF, IJ are parabola segments (uniformly decelerated motion), because only dry friction force acts on the body at these time intervals.

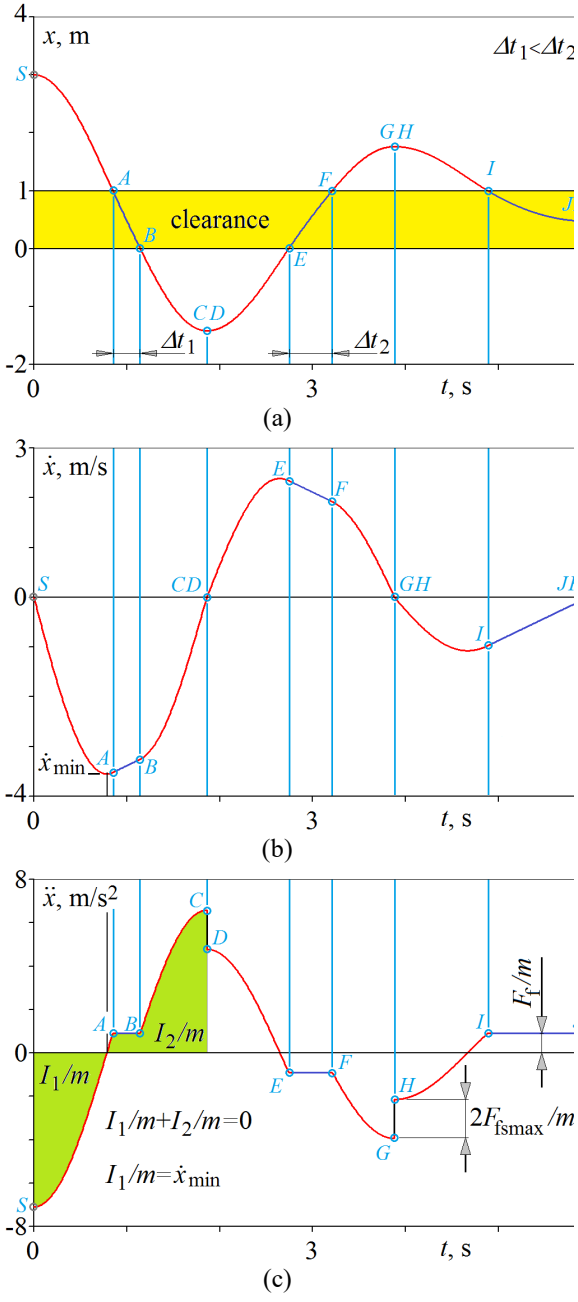

FIGURE 6. Time histories obtained for the system with clearance and Coulomb friction, calculated for the following data: m=1kg, k_1=k_2=4 N/m, l=1 m, c=0 N/(m/s), F_{fsmax}=0.9 N, $x_{(t=0)}$=3 m, $dx/dt_{(t=0)}$=0 m/s.

Whereas segments *SA*, *BC*, *DE*, *FG*, *HI* are sinus segments. This shows, that the exact piecewise-defined function is known, but identification of non-linearity from the time history of displacement is difficult. Next time history of velocity is studied (Fig. 6b). In this case extremes have characteristic shape, and function is not smooth in points *CD*, *GH* and *JK* ($dx/dt=0$). As a result, time history of acceleration is discontinuous in these points (*CD*, *GH*, *JK*) (Fig. 6c). These jump discontinuities appear due to Coulomb friction, which can be identified from this graph. Moreover, straight line segments appear between points *AB*, *EF*, *IJ*, which reflect both clearance and Coulomb friction. Finally, two impulses I_1 and I_2 are presented. Summarizing, time history of acceleration well reveals non-linearity in contrast to time history of displacement.

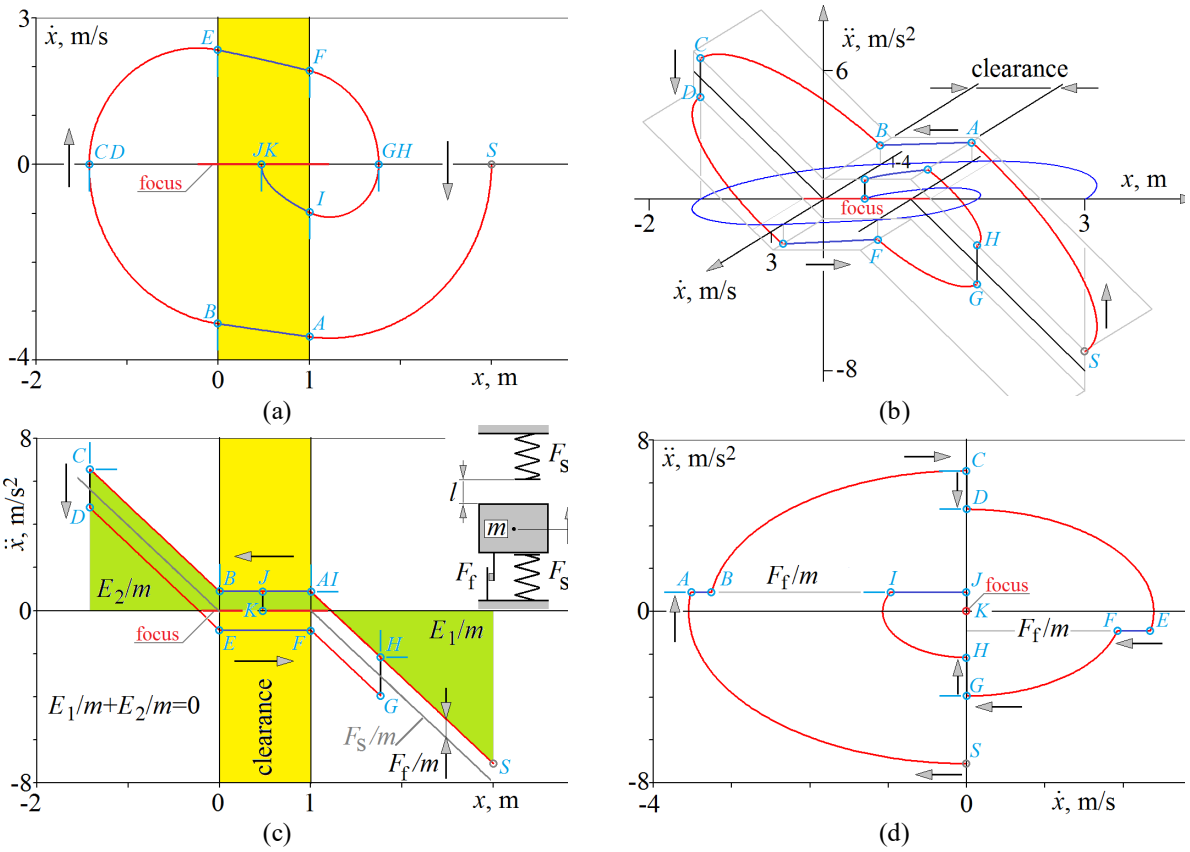

FIGURE 7. Trajectories obtained for the system with clearance and Coulomb friction, for the following data: m=1kg, $k_1=k_2$=4 N/m, l=1 m, c=0 N/(m/s), F_{fsmax}=0.9 N, $x_{(t=0)}$=3 m, $dx/dt_{(t=0)}$=0 m/s.

After that, trajectories are studied. In this case focus is observed, which is a segment (Fig. 7c). It should be noted, that focus is longer than l, and all equilibrium positions are stable. *AB, EF* and *IJ* segments are straight line segments, and they reflect clearance and dry friction force ($d^2x/dt^2=F_f/m$). Whereas vertical segments *CD*, *GH* and *JK* reflect jump of dry friction. Effects of acting forces are observed, and thus the forces can be identified from x-d^2x/dt^2 trajectory [7]. Potential energy is dissipated by Coulomb friction, hysteresis loop is evident, and thus amplitude drops. Moreover energy flow is observed $E_1=E_2$. This trajectory provides a lot of information (Fig. 7c). Then, x-dx/dt trajectory is studied (Fig. 7a). This trajectory contains square root segments (*AB*, *EF*, *IJ*) and segments of ellipse (*SA*, *BC*, *DE*, *FG*, *HI*). Next, dx/dt-d^2x/dt^2 trajectory reveals both clearance and dry friction; projection of *AB* segment is not a point, but is a segment, because dry friction reduces speed (Fig. 7d). Segments *AB, EF, IJ* are on two straight lines. Moreover, vertical segments reflect jump of friction force. Finally, the most interesting is 3D trajectory x-dx/dt-d^2x/dt^2, because presents all provided information (Fig. 5b). Point circulates along path *SABCD*... round focus on surfaces determined by acting forces $d^2x/dt^2=(F_s+F_f)/m$. Blue line presents x-dx/dt trajectory. This shows, that valuable information is evident on these trajectories.

Stopping conditions, are presented as a pseudo code:

$$\text{if } (\mathrm{d}x/\mathrm{d}t = 0 \text{ and } |F_s| < F_{fsmax}) \text{ then } \mathrm{d}^2x/\mathrm{d}t^2 = 0 \text{ else } \mathrm{d}^2x/\mathrm{d}t^2 = (F_s + F_f)/\mathrm{m} \,. \tag{9}$$

This part of code is very important during simulation, and is used in many areas. For example contact forces during car accidents are modeled with Hook and Saint-Venant's bodies [11]. Moreover, stopping conditions is used during car braking (points *IJK*).

CONCLUSIONS

Presented models describe mechanical systems, for example bearings, machine tools and guide ways. Usually, machine tools are modeled with linear models [12], whereas non-linear forces play a significant role. Clearance changes dynamics; natural frequency is a function of amplitude, and thus resonance phenomenon is changed. Moreover notions of center, focus and amplitude should be precisely defined. Then, dry friction introduces jump discontinuity of time history of acceleration. This shows, that simple non-linear models show sophisticated dynamics.

Trajectories provide valuable information about system, thus should be widely used. For example some non-linearities are evident, and parameters can be easily identified.

If linear models are studied, then these phenomena are neglected, thus non-linear models should be used. For better modeling machine tools dynamic, non-linear models with memory should be employed [13].

REFERENCES

1. R. Grzejda, "Modelling nonlinear multi-bolted connections: A case of the assembly condition" 15th International Scientific Conference on Engineering for Rural Development (Jelgava, Latvia May 25-27, 2016), pp. 329-335.
2. R. Grzejda, "Modelling nonlinear multi-bolted connections: A case of operational condition" 15th International Scientific Conference on Engineering for Rural Development (Jelgava, Latvia May 25-27, 2016), pp. 336-341.
3. A. Bisoffi, M. Da Lio, A.R. Teel and L. Zaccarian, IEEE Trans Automat Contr **63**, 2654–2661 (2018).
4. T. Piatkowski, Mech Mach Theory **73,** 91–100 (2014).
5. R. Kostek, Appl Math Comput **219**, 10082-10095 (2013).
6. J. Awrejcewicz, Vibration of discrete deterministic systems. (WNT, Warsaw, 1996).
7. R. Rułka, "Identification of spring and damping characteristic from free vibrations" 2nd Conference in Institute of Aviation (Warsaw, May 29- June 1, 1968), pp. 113-116.
8. S.F. Masri and T.K. Caughey, J Appl Mech-T ASME **46**, 433-447 (1979).
9. R. Kostek, "Simulation of non-linear vibrations to find state indicators" MSc thesis, ATR Bydgoszcz, 1998.
10. T. Dossogne, J.P. Noël, C. Grappasonni, G. Kerschen, B. Peeters, J. Debille, M. Vaes and J. Schoukens, "Nonlinear ground vibration identification of an F-16 aircraft Part II : understanding nonlinear behavior in aerospace structures using sine-sweep testing " International Forum on Aeroelasticity and Structural Dynamics, At Saint Petersburg, Russia, Proc. IFASD 2015".
11. R. Kostek and P. Aleksandrowicz, "Identification of the parameters of vehicle contact with a rigid barrier from a crash test" 23rd International Conference Engineering Mechanics 2017 (Svratka, Czech Republic, 15 – 18 May 2017), pp. 494 – 497.
12. K. Marchelek, Machine tool dynamics (WNT, Warsaw, 1991).
13. R. Kostek, J Theor App Mech-Pol **50**, 509-530 (2012).